Published OnlineFirst September 12, 2013; DOI: 10.1158/1078-0432.CCR-13-0527

Clinical Cancer Research

The mTOR Kinase Inhibitors, CC214-1 and CC214-2, Preferentially Block the Growth of EGFRvIII-Activated Glioblastomas

Beatrice Gini, Ciro Zanca, Deliang Guo, et al.

Clin Cancer Res 2013;19:5722-5732. Published OnlineFirst September 12, 2013.

Published OnlineFirst September 12, 2013; DOI: 10.1158/1078-0432.CCR-13-0527

Cancer Therapy: Preclinical

Clinical Cancer Research

The mTOR Kinase Inhibitors, CC214-1 and CC214-2, Preferentially Block the Growth of EGFRvIII-Activated Glioblastomas

Beatrice Gini[1,3], Ciro Zanca[1], Deliang Guo[13], Tomoo Matsutani[1], Kenta Masui[1], Shiro Ikegami[1], Huijun Yang[1], David Nathanson[1], Genaro R. Villa[1,10,11], David Shackelford[1], Shaojun Zhu[1], Kazuhiro Tanaka[1], Ivan Babic[1], David Akhavan[1], Kelly Lin[1], Alvaro Assuncao[1], Yuchao Gu[1,10], Bruno Bonetti[14], Deborah S. Mortensen[4], Shuichan Xu[4], Heather K. Raymon[4], Webster K. Cavenee[1,2,3], Frank B. Furnari[1,2,3], C. David James[5], Guido Kroemer[15,16,17,18,19], James R. Heath[6], Kristen Hege[12], Rajesh Chopra[12], Timothy F. Cloughesy[7,8,9], and Paul S. Mischel[1,2,3]

Abstract

Purpose: mTOR pathway hyperactivation occurs in approximately 90% of glioblastomas, but the allosteric mTOR inhibitor rapamycin has failed in the clinic. Here, we examine the efficacy of the newly discovered ATP-competitive mTOR kinase inhibitors CC214-1 and CC214-2 in glioblastoma, identifying molecular determinants of response and mechanisms of resistance, and develop a pharmacologic strategy to overcome it.

Experimental Design: We conducted *in vitro* and *in vivo* studies in glioblastoma cell lines and an intracranial model to: determine the potential efficacy of the recently reported mTOR kinase inhibitors CC214-1 (*in vitro* use) and CC214-2 (*in vivo* use) at inhibiting rapamycin-resistant signaling and blocking glioblastoma growth and a novel single-cell technology—DNA Encoded Antibody Libraries—was used to identify mechanisms of resistance.

Results: Here, we show that CC214-1 and CC214-2 suppress rapamycin-resistant mTORC1 signaling, block mTORC2 signaling, and significantly inhibit the growth of glioblastomas *in vitro* and *in vivo*. EGFRvIII expression and PTEN loss enhance sensitivity to CC214 compounds, consistent with enhanced efficacy in strongly mTOR-activated tumors. Importantly, CC214 compounds potently induce autophagy, preventing tumor cell death. Genetic or pharmacologic inhibition of autophagy greatly sensitizes glioblastoma cells and orthotopic xenografts to CC214-1- and CC214-2–induced cell death.

Conclusions: These results identify CC214-1 and CC214-2 as potentially efficacious mTOR kinase inhibitors in glioblastoma, and suggest a strategy for identifying patients most likely to benefit from mTOR inhibition. In addition, this study also shows a central role for autophagy in preventing mTOR-kinase inhibitor-mediated tumor cell death, and suggests a pharmacologic strategy for overcoming it. *Clin Cancer Res; 19(20); 5722–32. ©2013 AACR.*

Introduction

Glioblastoma is the most common malignant primary brain cancer in adults and one of the most lethal of all cancers (1). Phosphoinositide 3-kinase (PI3K) signaling is hyperactivated in approximately 90% of glioblastomas, commonly in association with EGF receptor (EGFR) amplification and mutation, and loss of the PTEN tumor suppressor protein (2, 3). The mTOR kinase—which links growth factor

Authors' Affiliations: [1]Laboratory of Molecular Pathology, Ludwig Institute for Cancer Research; [2]Moores Cancer Center; [3]University of California San Diego, La Jolla; [4]Celgene Corporation, San Diego; [5]Department of Neurological Surgery and Brain Tumor Research Center, University of California at San Francisco, San Francisco; [6]California Institute of Technology, Pasadena; [7]Henry Singleton Brain Tumor Program; [8]Jonsson Comprehensive Cancer Center; [9]Department of Neurology, David Geffen UCLA School of Medicine; [10]Department of Molecular and Medical Pharmacology; [11]UCLA Medical Scientist Training Program, University of California, Los Angeles, Los Angeles, California; [12]Celgene Corporation, Summit, New Jersey; [13]Department of Radiation Oncology, Ohio State University Comprehensive Cancer Center and Arthur G. James Cancer Hospital, Columbus, Ohio; [14]Department of Neurological, Neuropsychological, Morphological and Movement Sciences, University of Verona, Verona, Italy; [15]INSERM; [16]Metabolomics Platform, Institut Gustave Roussy, Villejuif; [17]Université Paris Descartes/Sorbonne Paris Cité; [18]Equipe 11 labellisée Ligue contre le Cancer, Centre de Recherche des Cordeliers; and [19]Pôle de Biologie, Hôpital Européen Georges Pompidou, Paris, France

Note: Supplementary data for this article are available at Clinical Cancer Research Online (http://clincancerres.aacrjournals.org/).

C. Zanca, D. Guo, and T. Matsutani contributed equally to this work.

Corresponding Author: Paul S. Mischel, Laboratory of Molecular Pathology, Ludwig Institute for Cancer Research, University of California at San Diego, 9500 Gilman Drive, La Jolla, California 92093, USA. Phone: +1-858-534-6080; Fax: +1-858-534-7750; E-mail: pmischel@ucsd.edu

doi: 10.1158/1078-0432.CCR-13-0527

Published OnlineFirst September 12, 2013; DOI: 10.1158/1078-0432.CCR-13-0527

Translational Relevance

Despite the compelling nature of mTOR as a drug target in glioblastoma, the allosteric inhibitor rapamycin has failed to show benefit for patients of glioblastoma, potentially because of a failure to fully suppress mTOR signaling. Here, we show that the newly described ATP-competitive mTOR kinase inhibitors CC214-1 and CC214-2 suppress rapamycin-resistant mTORC1 signaling, block mTORC2 signaling, and significantly inhibit the growth of glioblastomas *in vitro* and *in vivo*; in addition, we identify EGFRvIII and PTEN loss as molecular determinants of response. We further show autophagy as a resistance mechanism, which can be overcome with the addition of chloroquine. Taken together, this study identifies potentially efficacious new mTOR kinase inhibitors, couples it to a strategy to direct it to patients most likely to benefit, and suggests a combinatorial pharmacologic approach to suppress autophagy-dependent drug resistance.

receptor signaling through PI3K with protein translation, proliferation, and survival—is, therefore, frequently hyperactivated in many cancer types, including the majority of glioblastomas (4, 5). mTOR functions through two well-described multiprotein complexes: mTORC1, which promotes many of its cellular activities through phosphorylation of S6 kinase and 4E-BP1, and mTORC2, which phosphorylates Akt to maximize its activity (5). Despite the central importance of mTOR signaling in glioblastoma, the allosteric mTORC1 inhibitor rapamycin has been shown to be ineffective in patients with glioblastoma (6, 7). Recent work from our group shows that this is mediated, at least in part, by failure to suppress mTORC2 signaling (6). Further, rapamycin has also been shown to be ineffective at durably suppressing 4E-BP1 phosphorylation in certain cellular contexts, suggesting that rapamycin-resistant mTORC1 signaling may also underlie clinical failure (8, 9).

ATP-competitive mTOR kinase inhibitors, which could potentially suppress rapamycin-resistant mTORC1 and mTORC2 signaling, have the potential to improve the treatment of patients with glioblastoma. However to date, their efficacy, molecular determinants of sensitivity, and potential mediators of resistance are not understood. Here, we conduct a series of *in vitro* and *in vivo* studies in glioblastoma cell lines to determine the potential efficacy of the recently reported mTOR kinase inhibitors CC214-1 (*in vitro* use) and CC214-2 (*in vivo* use) at inhibiting rapamycin-resistant signaling and blocking glioblastoma growth (10). We identify molecular determinants of sensitivity, and show that autophagy plays a central role in preventing CC214-mediated cell death, which can be reversed by genetic or pharmacologic inhibition of autophagy. These results identify CC214-1 and CC214-2 as potentially effective agents, particularly in combination with lysosomotropic, autophagy-inhibitory compounds.

Materials and Methods

Cell lines and reagents

The U87, U87EGFRvIII, U87EGFR, and U87EGFRvIII/-PTEN cells were obtained as previously described (5); U251 and LN229 were cultured in Dulbecco's modified Eagle's medium (DMEM; Cellgro) supplemented with 10% FBS (vol/vol, Omega Scientific) and 100 U/mL penicillin and streptomycin (Gibco); the U373 Tet OFF system was kindly provided by the Webster Cavenee group (Ludwig Inst., San Diego, CA); the LN229 Tet ON cell lines were grown as described in the work by Guo and colleagues (11). GBM39 primary neurospheres were provided by Prof. David James (University of California at San Francisco, San Francisco, CA). All cell lines were cultured in a humidified 5% CO_2 (vol/vol) incubator, at 37°C. CC214-1 and CC214-2 were provided by Celgene Corporation (San Diego, CA). The development of the series that led to CC214 compounds (12) and its structure (10) have been described previously. P-Akt Ser473, P-Akt Thr308, P-NDRG1 Thr346, P-S6 Ser235/236, S6, cleaved PARP, P-4E-BP1 Thr37-46, 4E-BP1, eIF4E, LC3B, Atg-5, and Atg-5/12 antibodies were purchased from Cell Signaling Technologies. P-EGFR Tyr1086 and P-PRAS40 Thr246 were from Invitrogen. EGFRvIII was made by Dako. Actin, p62, and PTEN antibodies were purchased, respectively, from Novus Biologicals, Progen Biotechnik, and Cascade BioScience. Chloroquine was from Sigma.

Immunoblotting

Western blot analysis was conducted using a 10 to 50 μg range of total protein lysates. Lysates were obtained from cultured cells or snap-frozen tissues using radioimmunoprecipitation assay (RIPA) buffer (Boston BioProducts) and protease plus phosphatase inhibitor cocktail (Thermo Scientific). Monodimensional electrophoresis was applied in 4% to 12% gradient gels NuPAGE Bis–Tris Mini Gel (Invitrogen); 10% or 15% acrylamide (vol/vol; National Diagnostics) gels were made and used to improve middle- and low-molecular weight (MW) protein separation. Proteins have then been transferred on nitrocellulose membranes (GE Healthcare), using a BioRad transfer chamber, applying 110 Volts for 1 hour. Membranes were subsequently blocked in Tris-buffered saline containing 0.1% Tween20 (vol/vol) and 5% BSA (g/mL; Fischer Scientific) for 1 hour. Primary antibody incubations were conducted overnight, at 4°C. Incubation with secondary horseradish peroxidase (HRP)-conjugated antibodies was done at room temperature (RT) for 1 hour. Detection of the immunoreactivities was obtained with Super Signal West Pico Chemiluminescent Substrate or West Femto Trial kit (Thermo Scientific). Scanned films or digitalized images acquired by Chemidoc (BioRad), Image Lab 4.0.1, were quantified using Image J software (NIH).

Cell proliferation

Water Soluble Tetrazolium (WST) assay was conducted with the Cell Proliferation Assay Kit (Chemicon). Specifically, cells were seeded at a density of 1×10^3 cells each well in 1% FBS DMEM (vol/vol), then a first reading after

Published OnlineFirst September 12, 2013; DOI: 10.1158/1078-0432.CCR-13-0527

adhesion was done; thereafter, drug treatment was started and continued for up to 4 days. On each day of reading, plates were incubated for 2 hours with tetrazolium salt WST 1 [2-(4-iodophenyl)-3-(4-nitrophenyl)-5-(2,4-disulfophenyl)-2H-tetrazolium, monosodium salt] (Chemicon) in the incubator. The absorbance was measured with a microplate reader (BioRad) at 420 to 480 nm.

Viability tests

Fifteen thousand glioblastoma cells were seeded in 12-well plates and treated, after one night, with CC214-1 at 0.1, 1, 2, 5, and 10 μmol/L. Chloroquine 10 μmol/L was used for combinatory treatment. Cell viability was evaluated after 3 days of treatment, and assessed by trypan blue exclusion (Invitrogen).

Flow cytometry analysis: Annexin V, PI

Viability was assessed in glioblastoma cell lines with the Annexin V, PI kit (BD), according to the manufacturer's instructions, after 72 hours of CC214-1 (2 μmol/L) treatment.

In vivo experiments

Flank xenografts. U87EGFRvIII xenografts models were obtained in full compliance with the University of California Los Angeles (UCLA)-Division of Laboratory Animal Medicine (DLAM) regulation and after approval by the Chancellor's Animal Research Committee of UCLA. In particular, U87-EGFRvIII cells were implanted subcutaneously in immunocompromised nonobese diabetic severe-combined immunodeficient (NOD/SCID)-γ null mice. Cells were cultured, trypsinized, and resuspended in PBS (Cellgro) plus Matrigel (BD Biosciences), as a 1:1 solution, at 6×10^6 cells/mL density. Tumor sizes were monitored daily using automated caliper. CC214-2 treatment, 50 mg/kg, was done by oral gavage, once every day in a suspension containing 0.5% carboxymethylcellulose (g/mL, Sigma), 0.25% Tween-80 (vol/vol; Sigma) in nanopure water. Mice were euthanized when tumors reached 15 mm diameter.

Orthotopic xenografts. U87EGFRvIII-TurboFP635 orthotopic xenografts models were obtained in full compliance with the University of California San Diego (UCSD)-Institutional Animal Core and Use Committee (IACUC).

Plasmid and cells. TurboFP635 fluorescent protein was used to tag U87EGFRvIII cells that were injected intracranially. Briefly, the lentiviral LV plasmid (13) was digested with NheI and XhoI. The same restriction enzymes were used to subclone the far-red fluorescent TurboFP635 protein sequence in the vector (Evrogen JSC). The lentivirus was obtained by transient transfection of 293T cells. The U87EGFRvIII cells were then infected with the virus carrying the sequence for the far-red protein TurboFP635 and subjected to two cycles of fluorescence-activated cell sorting (FACS) to sort and enrich the most fluorescent 5% cell population in each cycle.

Intracranial injection procedure. A total of 1×10^5 U87EGFRvIII cells, tagged with the far-red protein TurboFP635 in a 5 μL volume, were injected intracranially into 4-week-old athymic nude mice using a stereotactic system according to the protocol described by Lee and colleagues (14). *In vivo* tumors were measured using near-infrared quantitative fluorescence imaging by fluorescence molecular tomography (FMT; FMT 2500, PerkinElmer). Tumor fluorescence emission, at 635 nm, was collected on the first day of treatment and on the day the animals were sacrificed. CC214-2 treatment, at 100 mg/kg, was done by oral gavage, once every 2 days in a suspension containing 0.5% carboxymethylcellulose (g/mL; Sigma), 0.25% Tween-80 (vol/vol, Sigma) in nanopure water. Chloroquine, 30 mg/kg in nanopure water, was administered intraperitoneally, once every 2 days. Mice were euthanized in accordance with the UCSD Institutional Guidelines for Animal Welfare and Experimental Conduct. Survival until the onset of neurologic sequelae in the vehicle mice was considered to determine the time of sacrifice.

Immunohistochemistry and immunofluorescence

Paraffin-embedded U87EGFRvIII xenografts blocks were sectioned at the UCLA Pathology Histology and Tissue Core Facility and at the UCSD Histology and Immunohistochemistry Shared Resource. Immunohistochemistry (IHC) was conducted as described by Mellinghoff and colleagues (15). Three images per IHC slide were captured using a DP 26 camera mounted on an Olympus BX43 microscope at ×40 magnification. Quantitative analysis of the IHC-stained slides was conducted with the image-analyzing software Microsuite Five (Olympus). Immunofluorescence staining was done as previously described in Gini and colleagues (16).

Cap-binding proteins assay

U87EGFRvIII cells were treated with CC214-1 (2 μmol/L) or rapamycin (5 nmol/L) for 24 hours. Five hundred microgram of protein lysates from control and treated cells, obtained as described in the "Immunoblotting," were incubated with 7-Methyl GTP Sepharose (GE Healthcare) for 4 hours at 4°C, on a rotating shaker. Resin was then centrifuged for 90 seconds at 1,800 rpm and pellet-washed twice with RIPA buffer. Resin was further incubated for 5 minutes at 99°C with loading buffer 2×. After centrifugation, cap-binding proteins were collected in the supernatant and analyzed by immunoblotting.

Capture of EGFR, EGFRvIII-positive cells by DNA-encoded antibody library

Capture of EGFR, EGFRvIII-positive cells from GBM39 neurospheres has been conducted by DNA encoded antibody library (DEAL) as described in Bailey and colleagues (17). Briefly, DEAL array (CalTech) was blocked with 1% BSA solution (g/mL) for 30 minutes, washed in PBS and deionized water, and then incubated with oligo-cetuximab (Bristol–Myers) conjugate for 30 minutes, at 37°C. The array was washed with 0.1% BSA in PBS (g/mL), and a single-cell suspension of GBM39 cells was applied on it for

Published OnlineFirst September 12, 2013; DOI: 10.1158/1078-0432.CCR-13-0527

40 minutes, in ice. After washing, the array of cells was used for immunofluorescence assay.

Short hairpin RNA assay

Escherichia coli carrying sh-Atg-5 pLKO.1 plasmids (Sigma) were expanded in LB medium (Fisher Scientific) and then the plasmids were extracted using MidiPrep kit (Qiagen). For lentiviral production, 293T cells were transfected with sh-Atg-5 pLKO.1 or sh-scramble pLKO.1, together with packaging, envelope plasmids, and polybrene (Sigma). Viral harvesting was achieved after 2 days from transfection, in high BSA growth medium. Sixty-thousand U87EGFRvIII cells were seeded in 6-cm plates and infected over night with lentivirus carrying sh-Atg5 or sh-scramble

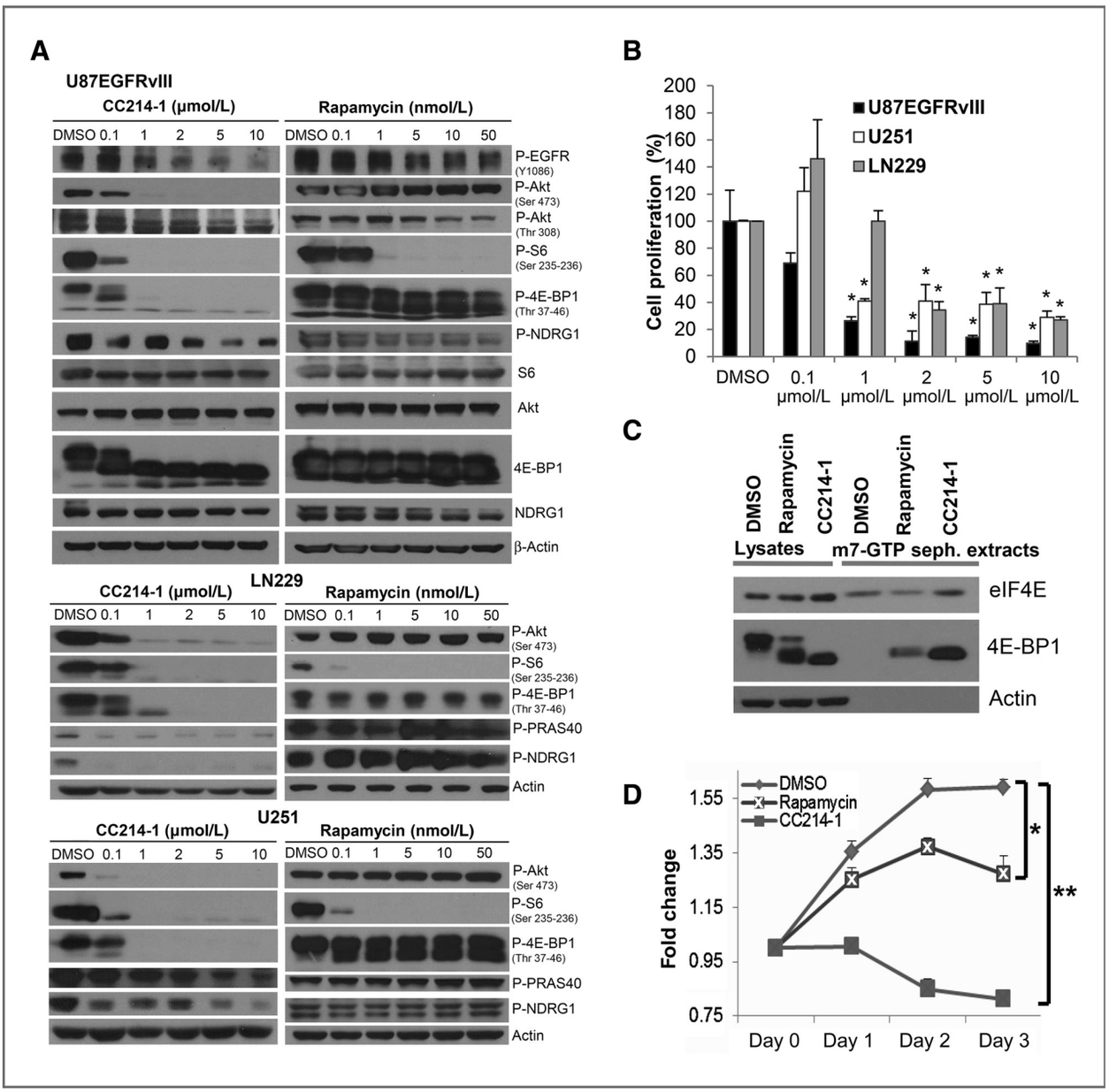

Figure 1. A, CC214-1 induces potent mTORC1/mTORC2 inhibition and tumor growth reduction in glioblastoma cell lines *in vitro*. Immunoblotting analysis of mTORC1/2 effectors activities, after 8 hours of treatment with CC214-1 or rapamycin at increasing concentrations, in U87EGFRvIII, LN229, and U251 glioblastoma cell lines. B, cellular proliferation in three glioblastoma cell lines as assessed by trypan blue exclusion cell count and normalized to dimethyl sulfoxide (DMSO) control. U87EGFRvIII proved to be the most sensitive glioblastoma cell line assessed, with IC_{50} in the 0.5 μmol/L range (B). C, inhibition of cap-dependent translation by CC214-1 (2 μmol/L) or rapamycin (5 nmol/L), was assessed by the level of 4E-BP1 bound to the 5′-cap in U87EGFRvIII cell lysates after 24 hours of treatment. D, WST proliferation experiment in U87EGFRvIII cells comparing DMSO, CC214-1 (2 μmol/L) and rapamycin (5 nmol/L) treatments. (P-S6, P-4E-BP1 have been selected as the mTORC1 biomarker's activity; P-Akt-S473, P-PRAS40, and P-NDRG1 were the selected mTORC2 effectors). *, $P < 0.05$; **, $P < 0.0001$ (Student *t* test). Data represent average of three independent experiments.

Published OnlineFirst September 12, 2013; DOI: 10.1158/1078-0432.CCR-13-0527

plasmids. Selection of sh-positive cells was achieved after 10 days of growth in medium containing puromycin (2 μg/mL; Sigma).

Crystal violet analysis

Twenty thousand U87EGFRvIII sh-scramble and U87EGFRvIII sh-Atg5 cells were seeded in six-well plates under puromycin selection. After 3 days of incubation in CC214-1, 2 μmol/L, cells were shortly air dried, fixed for 5 minutes in ParaFormAldehyde (PFA) 4% (vol/vol; Santa Cruz Biotechnology) and stained in 0.05% crystal violet (g/mL; Sigma) solution for 30 minutes. Plates were then washed twice with tap water and air dried for 2 minutes. Pictures of the plates were taken using a Nikon Eclipse TS100 scope equipped Canon S51S camera.

Results

CC214-1 inhibits rapamycin-resistant mTORC1 and mTORC2 signaling, limits protein translation, and blocks glioblastoma cell proliferation

We examined the biochemical and antiproliferative effect of CC214-1 on a panel of glioblastoma cell lines (Fig. 1A and B; Supplementary Fig. S1). CC214-1 dose-dependently inhibited mTORC1 signaling in all glioblastoma cell lines tested, potently suppressing rapamycin-resistant 4E-BP1 and mTORC2 signaling, as shown by effects on 4E-BP1 (Thr 37-46), and Akt (Ser 473), PRAS40 (Thr 246), and NDRG-1 (Thr 346) phosphorylation, respectively (Fig. 1A; Supplementary Fig. S1). This was confirmed even in the presence of a rapamycin concentration 10 times higher (50 nmol/L) than the minimal effective dose (5 nmol/L) that inhibits mTORC1 (Fig. 1A). Consistent with the enhanced inhibition of 4E-BP1 phosphorylation, CC214-1 showed markedly suppressed m^7G cap-dependent translation relative to rapamycin, indicating that the dual mTOR kinase inhibitor was significantly more efficacious at blocking mTOR-dependent protein translation (Fig. 1C). Further, CC214-1 was significantly more effective than rapamycin at blocking glioblastoma cell proliferation in culture (Fig. 1D). We have recently shown that ATP-competitive mTOR kinase inhibitors synergize with rapalogs (18). Consistent with these findings, CC214-1 synergized with rapamycin, inhibiting mTORC1 signaling and tumor cell proliferation at subtherapeutic doses of each compound (Supplementary Fig. S2A).

EGFRvIII expression and PTEN loss sensitize tumor cells to CC214-1

To test the hypothesis that EGFR activation promotes sensitivity to CC214-1, we examined the impact of EGFRvIII or EGF-stimulation of wild-type EGFR, in isogenic glioblastoma cell lines. Biochemical analyses confirmed that CC214-1 successfully inhibited mTORC1-dependent 4E-BP1 and S6 phosphorylation in EGFRvIII-expressing glioblastoma cells (Fig. 2A–C; Supplementary Figs. S2B and S3A), as well as blocked EGF-induced 4E-BP1 and S6 phosphorylation in glioblastoma cells overexpressing wild-type EGFR (Supplementary Fig. S3B). Further, CC214-1 showed superior inhibition of P-Akt (Ser 473), P-S6 (Ser 235-236), and P-

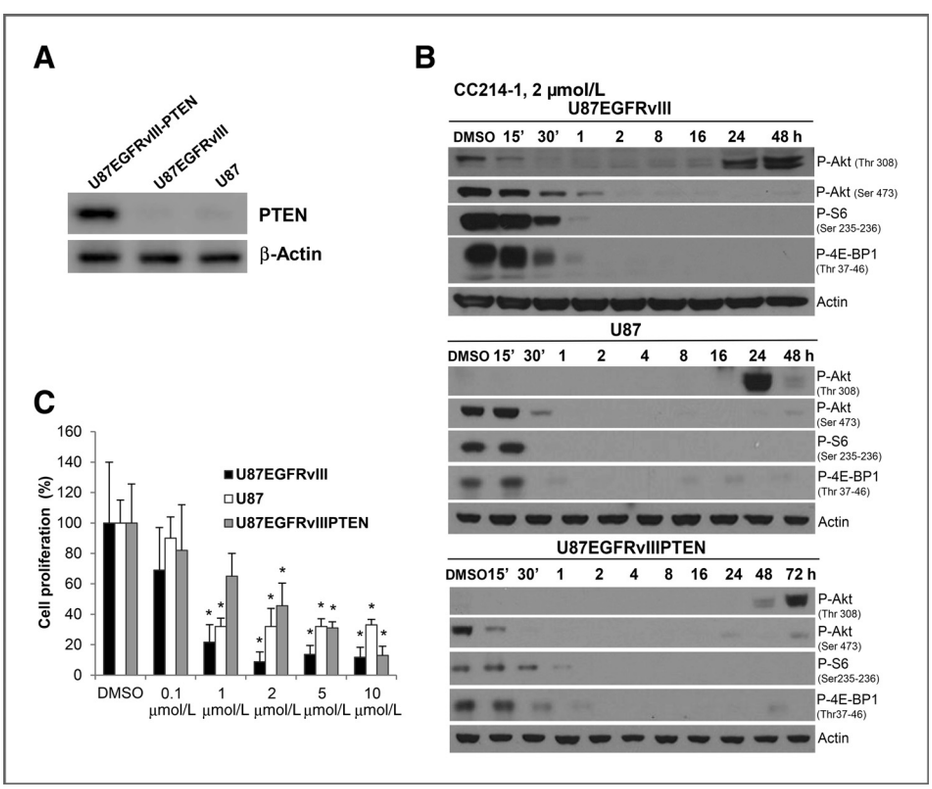

Figure 2. A, EGFRvIII expression and PTEN loss sensitize glioblastoma cells to CC214-1–dependent inhibition of proliferation. CC214-1 efficacy has been evaluated in a panel of isogenic U87 cell lines differentially expressing EGFRvIII and PTEN. B, reduction of mTORC1 and mTORC2 biomarkers followed CC214-1 treatment (2 μmol/L) was observed in all of the three cell lines by Western blot. C, cellular proliferation in three isogenic U87 cell lines as assessed by trypan blue exclusion cell count after treatment with CC214-1 and normalization to DMSO control. The EGFRvIII-positive and PTEN-negative U87 cell line (U87EGFRvIII) proved to be the most sensitive, when compared with EGFRvIII-negative, PTEN-negative cells (U87), or EGFRvIII-positive, PTEN-positive cells (U87EGFRvIIIPTEN) (C). Data represent average of three independent experiments. *, $P < 0.05$ (Student t test).

Published OnlineFirst September 12, 2013; DOI: 10.1158/1078-0432.CCR-13-0527

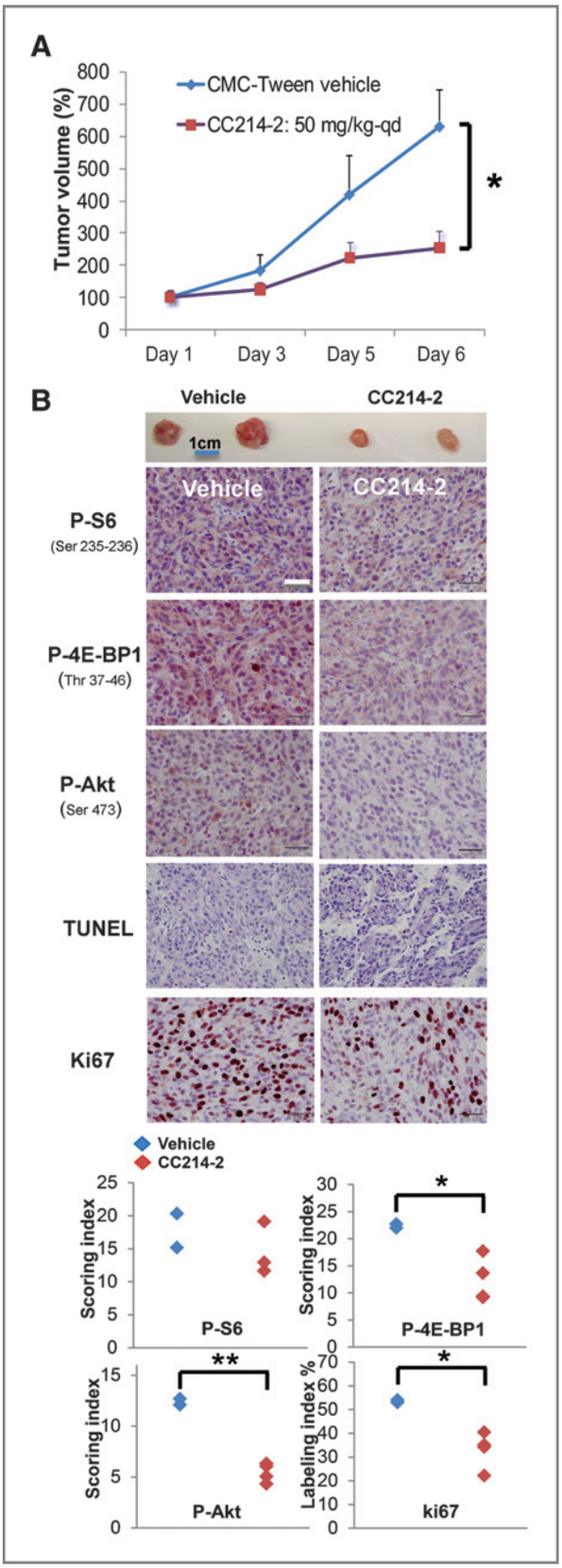

4E-BP1 (Thr 37-46) phosphorylation relative to any of the other EGFR, PI3K, or mTOR inhibitors tested (Supplementary Fig. S3B). Importantly, EGFRvIII sensitized U87 glioblastoma cells to CC214-1–mediated growth inhibition (Fig. 2C), an observation that was validated in another isogenic cell system, U373 glioblastoma cells, in which EGFRvIII was under the control of a tetracycline-regulated promoter (Supplementary Fig. S4A). PTEN reconstitution rendered glioblastoma cells less sensitive, despite similar levels of pathway inhibition (Fig. 2C). We used a novel technology, DEAL (19), to capture and analyze individual EGFRvIII expressing tumor cells from the heterogeneous patient-derived glioblastoma model, GBM39, in which individual tumor cells varied in EGFRvIII and PTEN expression (20). GBM39 cells were treated with CC214-1 in neurosphere cultures, after which the EGFR- and EGFRvIII-positive tumor cells were sorted using cetuximab-conjugated oligonucleotides and captured on a glass slide arrayed with their complementary oligonucleotide barcodes (Supplementary Fig. S2C). Immunofluorescent stain for PTEN was then conducted (Supplementary Fig. S2C). Consistently, in this patient-cell model, in which PTEN is heterogeneously expressed, a shift in the ratio of PTEN-positive/PTEN-negative cells was observed, with a significant increase in the percentage of PTEN-positive tumor cells in response to CC214-1 treatment relative to control. These data suggest a preferential effect of CC214-1 on the PTEN-deficient tumors, consistent with our studies in the isogenic U87-GBM cell lines. Taken together, these data suggest that EGFRvIII expression and PTEN loss sensitizes glioblastoma cells to CC214-1–mediated cell-growth arrest.

CC214 potently blocks tumor growth *in vivo*

We then assessed the potential of CC214-2, an analogue related to CC214-1 with pharmacokinetic properties suitable for *in vivo* application (10), to inhibit the growth of U87EGFRvIII cells *in vivo* (Fig. 3). CC214-2 significantly reduced the growth of U87EGFRvIII flank xenografts (Fig. 3A) by more than 50%, after 1 week of treatment via oral gavage. Immunohistochemical analysis showed mTORC1 and mTORC2 inhibition, as measured by diminished P-S6, P-4E-BP1, and P-Akt cytoplasmic staining (Fig. 3B). CC214-2 treatment resulted in markedly diminished Ki67 staining (Fig. 3B). In contrast, no change in terminal deoxynucleotidyl transferase–mediated dUTP nick end labeling

Figure 3. *In vivo* CC214-2 treatment of U87EGFRvIII flank xenografts downregulates mTORC1–mTORC2 effector's functions, and significantly reduces tumor proliferation. A, antitumor activity of CC214-2 in U87EGFRvIII flank xenograft models, after 6 days of oral dosing CC214-2 (50 mg/kg once a day) treatment resulted in greater than 50% tumor volume reduction. Representative xenografts are shown underneath the graph. B, immunohistochemistry on U87EGFRvIII xenograft's sections shows downregulation of the main mTORC1, mTORC2 biomarkers. TUNEL staining did not change between controls and treated samples, whereas Ki67, a marker for cell proliferation, was decreased upon CC214-2 treatment (B). P-S6 (Ser 235-236), P-4E-BP1 (Thr 37-46) denote mTORC1 effectors, P-Akt (Ser 473) represents mTORC2 activity. *, $P < 0.05$; **, $P < 0.01$; Student t test; $n = 2$ and $n = 4$ respectively for vehicle and CC214-2–treated flank xenografts; scale bar = 100 μm.

Published OnlineFirst September 12, 2013; DOI: 10.1158/1078-0432.CCR-13-0527

(TUNEL) staining was detected (Fig. 3B), indicating that CC214-2–mediated growth inhibition was due to its cytostatic effect, rather than a consequence of tumor cell death.

CC214-1 and -2 promote autophagy *in vitro* and *in vivo*

Inhibition of mTORC1 signaling has been linked to induction of autophagy, a state in which cells rely on intracellular degradative machineries to supply biomolecular building blocks to subvert stressful conditions (21). We hypothesized that induction of autophagy-enabled U87EGFRvIII glioblastoma cells to resist CC214-1 and -2–mediated cell death. To test this hypothesis, we examined the effect of CC214-1 on autophagy induction, and then determined its functional consequences using genetic and pharmacologic approaches. We first examined the level of LC3B-II and Atg5-12, which are recognized as autophagic biomarkers (Supplementary Fig. S4B). CC214-1 induced a transient expression of LC3B-II isoform and the conjugation of Atg12 to Atg5 indicative of the stimulation of the autophagy flux in U87EGFRvIII cell line (Supplementary

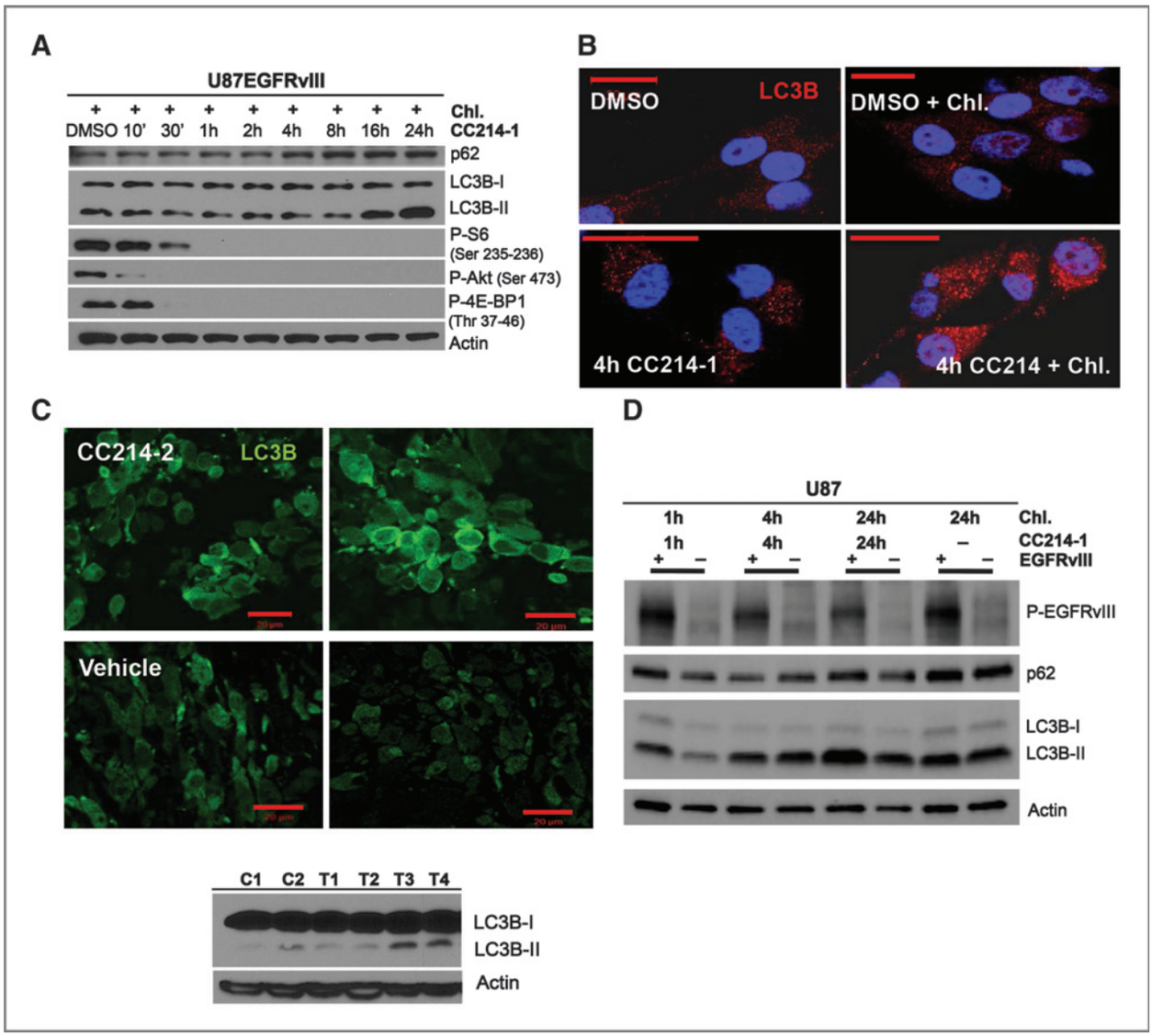

Figure 4. U87EGFRvIII glioblastoma cell line shows higher level of autophagy induction following CC214-1 exposure. A, time course experiment with CC214-1 (2 μmol/L) plus the autophagy inhibitor chloroquine (20 μmol/L), in U87EGFRvIII cells, reveals high degree of autophagic flux, registered as accumulation of LC3B-II, p62 proteins. B, immunofluorescent staining for LC3B protein in U87EGFRvIII cell line. CC214-1 treatment (2 μmol/L) shows typical intra-cellular autophagosomal puncta pattern (B). C, autophagy induction was registered also in CC214-2 treated (50 mg/kg qd, every day, for 6 days) U87EGFRvIII flank xenografts as indicated by the higher level of LC3B marker, in immunofluorescent staining (top) and immunoblotting (bottom), 24 hours after the last dose as compared with the vehicle control samples (LC3B staining for the CC214-2 and vehicle treated xenografts respectively in the two top and bottom photomicrographs; T= CC214-2 treated tumor; C= Vehicle treated tumor). D, time course experiment with CC214-1 (2 μmol/L) in U87EGFRvIII cells compared with U87 cell line shows that EGFRvIII sensitizes cells to CC214-1–mediated induction of autophagy, as shown by the major increase of LC3B protein and the higher p62 turnover. Chl., chloroquine. Scale bar: 20 μm.

Published OnlineFirst September 12, 2013; DOI: 10.1158/1078-0432.CCR-13-0527

Fig. S4B). Further, in the presence of chloroquine, which inhibits the late stages of autophagy by preventing degradation of autophagosome contents, CC214-1 treatment led to markedly elevated levels of LC3B-II and p62, consistent with CC214-1–mediated autophagy (Fig. 4A; Supplementary Fig. S4C). Immunofluorescence analysis highlighted enrichment of LC3B with localization into autophagosomes depicted as puncta (Fig. 4B). *In vivo*, CC214-2 similarly activated autophagy in U87EGFRvIII xenografts (Fig. 4C).

To determine whether EGFRvIII expression sensitized glioblastoma cells to CC214-mediated autophagy, we compared the level of autophagic flux in three different isogenic glioblastoma cell lines, with or without EGFRvIII expression. In U87 glioblastoma cells, or in U373 or LN229 glioblastoma cells in which EGFRvIII expression was under

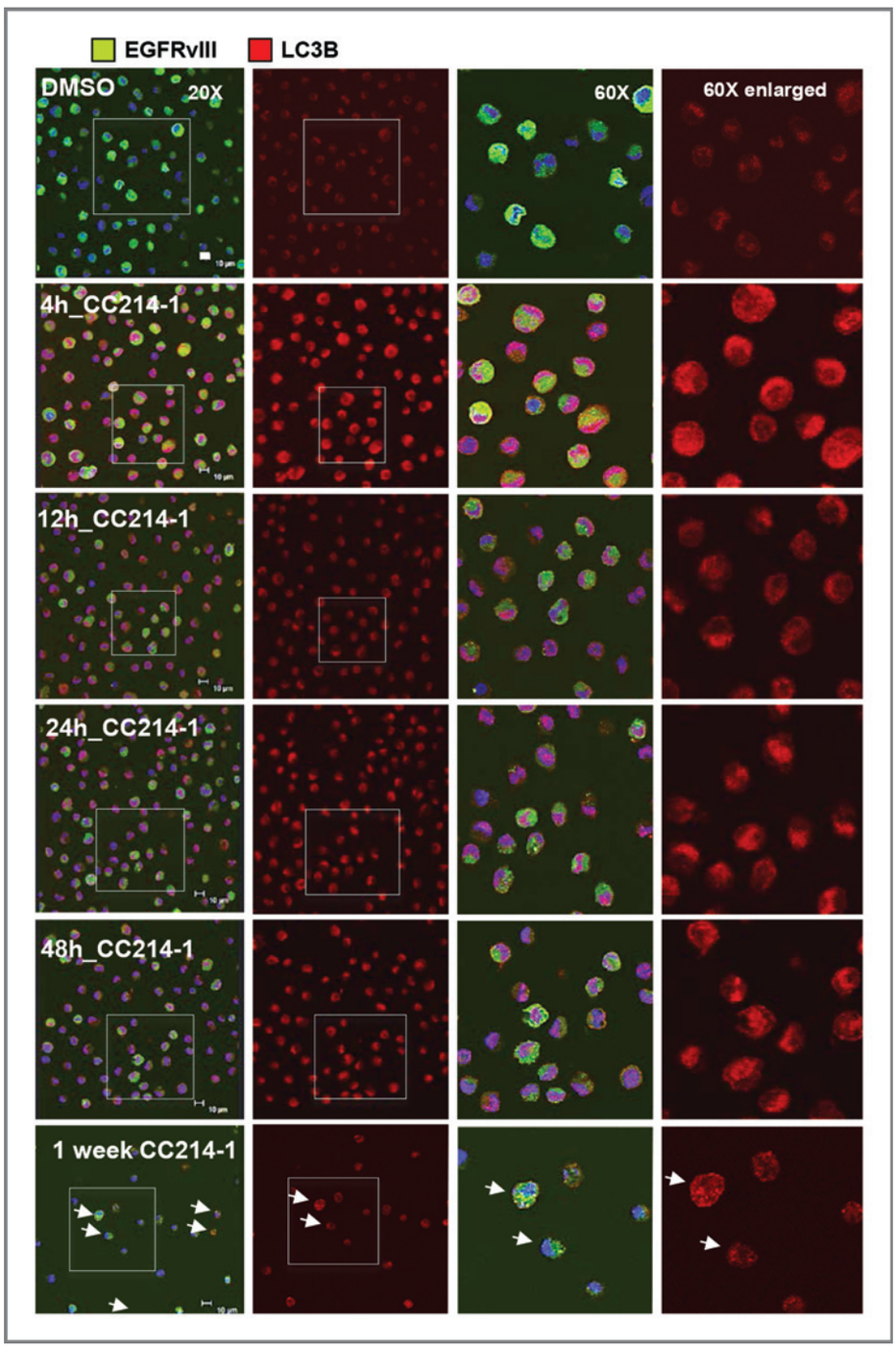

Figure 5. EGFRvIII-positive cells from the heterogeneous GBM39 primary neurospheres rely on autophagy as mechanism to resist to CC214-1 treatment. Double immunofluorescent staining for EGFRvIII (green) and LC3B (red) on DEAL-captured EGFR wt, EGFRvIII-positive GBM39 cells highlights the high level of staining of the autophagy marker LC3B in the EGFRvIII-positive cells (as indicated by the white arrows), upon CC214-1 (5 μmol/L) time course treatment (scale bar = 10 μm).

Published OnlineFirst September 12, 2013; DOI: 10.1158/1078-0432.CCR-13-0527

the control of a tetracycline-regulated promoter, EGFRvIII enhanced autophagic flux in response to CC214-1 treatment (Fig. 4D; Supplementary Fig. S5).

To further understand the role of endogenous EGFRvIII expression in promoting autophagic flux in response to mTOR kinase inhibition in glioblastoma, we used DEAL technology (19) to capture and analyze individual EGFRvIII-expressing tumor cells from the heterogeneous patient-derived glioblastoma model, GBM39 (20). GBM39 cells were treated with CC214-1 and the EGFR, EGFRvIII-positive tumor cells were captured by DEAL as previously described (Fig. 5). The captured glioblastoma cells were stained using double immunofluorescence for EGFRvIII and LC3B proteins (Fig. 5). The DEAL captured EGFRvIII-positive cell were highly positive for punctate LC3B immunostaining upon CC214-1 treatment (Fig. 5). Western blot analysis confirmed the induction of autophagy in GBM39 cells, characterized by massive lipidation of LC3B-I to LC3B-II isoform (Supplementary Fig. S6A).

These results raised the possibility that EGFRvIII, while sensitizing glioblastoma cells to mTOR kinase growth inhibition, may also protect them from cell death by engaging autophagy. High levels of autophagy have been previously described in oncogene-addicted tumor models, with activating mutations in Ras (22), and in glioblastoma cells treated with PI3K/mTOR kinase inhibitors (23). In fact, induction of autophagy has been shown to protect glioblastoma cells from PI3K/mTOR-kinase-inhibitor–induced tumor cell death in a chloroquine-reversible fashion (23). Therefore, we set out to use genetic and pharmacologic approaches to determine whether inhibition of autophagy could sensitize glioblastoma cells to CC214-1–dependent cell death. Chloroquine abrogated CC214-1–mediated autophagy, significantly sensitizing glioblastoma cells to CC214-1–dependent

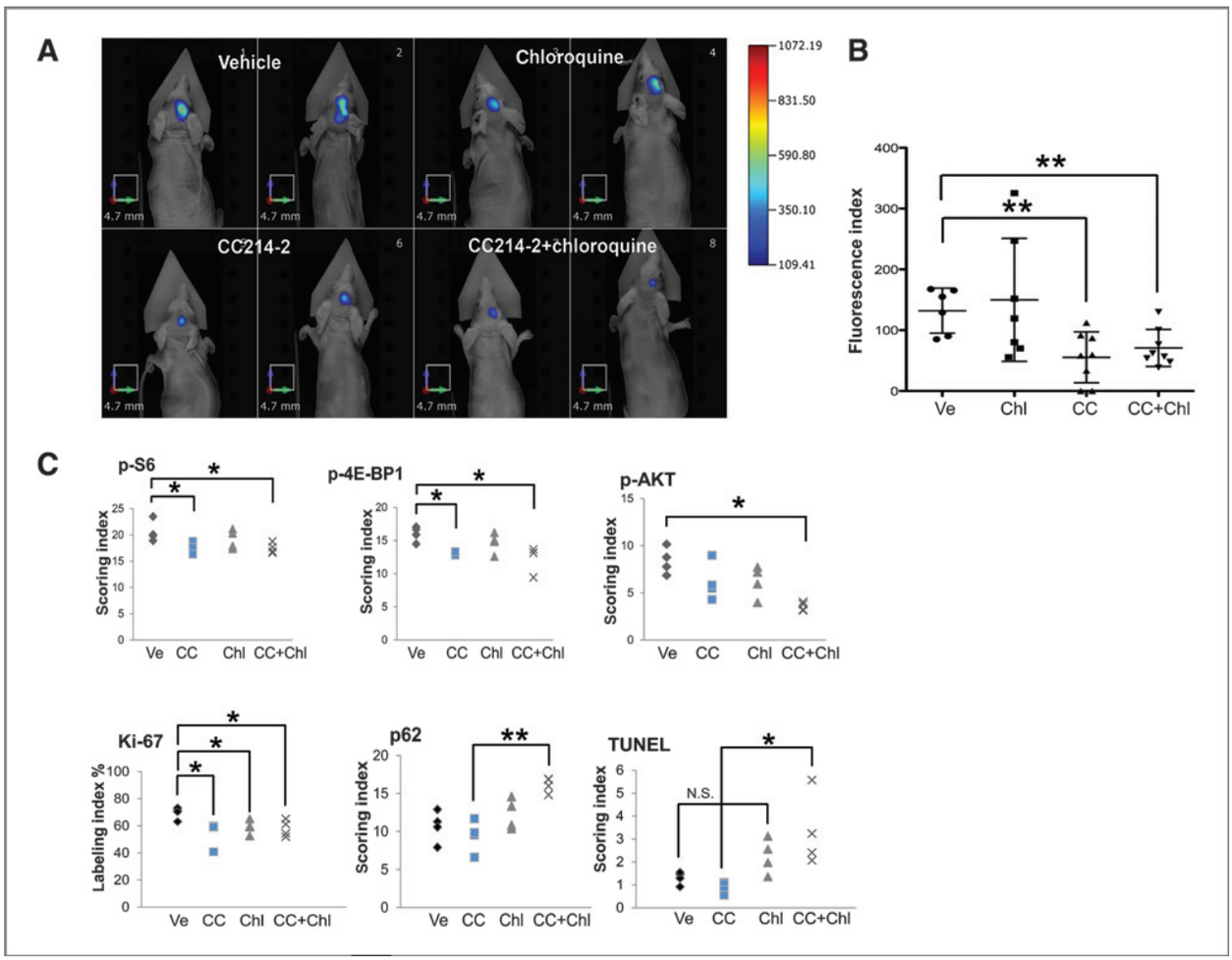

Figure 6. *In vivo* combinatory treatment in U87EGFRvIII orthotopic xenografts with CC214-2 and chloroquine significantly reduced tumor growth and induced tumor cell death. A, fluorescence molecular tomography (FMT) images showing the antitumor activity of CC214-2 in single treatment or in combination with chloroquine in U87EGFRvIII intracranial xenograft models, after 6 days of dosing. B, CC214-2 treatment resulted in greater than 50% reduction of tumor volume as assessed by FMT imaging. C, CC214-2 treatment significantly inhibited mTORC1 and mTORC2 signaling, and reduced the Ki67 proliferation index. C, chloroquine treatment suppressed autophagy, as measured by enhanced p62 staining, promoting tumor cell death (TUNEL-positive staining) of CC214-2–treated mice. *, $P < 0.05$; **, $P < 0.01$; Student *t* test ($n = 8$ for the orthotopic xenografts; CC214-2, 100 mg/kg, once every 2 days by gavage; chloroquine, 30 mg/kg, once every 2 days intraperitoneally; Ve, vehicle; CC, CC214-2; Chl., chloroquine).

Published OnlineFirst September 12, 2013; DOI: 10.1158/1078-0432.CCR-13-0527

cell death, particularly in EGFRvIII-expressing tumor cells (Supplementary Fig. S7A and S7B). Consistent with this model, genetic inhibition of autophagy achieved through ATG5 knockdown similarly sensitized glioblastoma cells to massive tumor cell death in response to CC214-1 (Supplementary Fig. S6B–S6D).

In an intracranial glioblastoma model, CC214-2 inhibits mTORC1 and mTORC2 signaling and suppresses tumor growth, and addition of chloroquine promotes tumor cell death

Finally, to assess the potential efficacy of mTOR kinase inhibition in an intracranial glioblastoma model, and to assess the relative benefit of combining pharmacologic inhibition of autophagy, we developed U87EGFRvIII intracranial xenografts in which the tumor cells were labeled with the far-red protein TurboFP635 to enable noninvasive FMT imaging (14). We then assessed the effect of mTOR kinase inhibition with CC214-2 (100 mg/kg once every 2 days by oral gavage for 6 days) on mTOR pathway inhibition and tumor growth, and we examined the effect of the autophagy inhibitor chloroquine (30 mg/kg once every 2 days by intraperitoneal injection), alone or in combination. CC214-2 treatment resulted in highly significant inhibition of intracranial glioblastoma growth, concomitant with significant inhibition of mTORC1 and mTORC2 signaling ($P < 0.05$), and significant inhibition of the Ki67 proliferation index ($P < 0.05$; Fig. 6A–C; Supplementary Fig. S7C). Chloroquine treatment had no effect on mTOR pathway inhibition or tumor growth as measured by FMT index (Fig. 6A–C), but did reduce the Ki67 index and elevated p62 staining ($P < 0.05$). Importantly, combined treatment with CC214-2 and chloroquine did not alter tumor mTOR pathway inhibition or additionally decrease tumor growth relative to CC214-2 alone; however, it did enhance p62 staining ($P < 0.01$), and significantly increased TUNEL staining ($P < 0.05$; Fig. 6; Supplementary Fig. S7C). Taken together, these results show that CC214-2 inhibits mTORC1 and mTORC2 signaling in an intracranial glioblastoma model, and suggests that inhibition of autophagy promotes cell death in response to CC214-2 treatment.

Discussion

mTOR is a critical nexus in tumor cells, linking growth factor receptor signaling through the PI3K–Akt signaling pathway, with protein translation, cellular metabolism, and nutrient and energy status (4, 24). However, the allosteric mTOR inhibitor rapamycin has failed in the clinic for patients with glioblastoma, potentially as a consequence of persistent mTORC2 signaling (6) and because of the inability of rapamycin to durably suppress 4E-BP1 phosphorylation (8, 25). The findings presented here suggest that ATP-competitive mTOR kinase inhibitors such as CC214-1 and CC214-2 may be more effective than rapamycin because of their ability to suppress mTORC2 signaling and mTORC1-dependent 4E-BP1 phosphorylation.

Currently, the molecular determinants of mTOR kinase inhibitors are not well understood. Our data show that EGFRvIII, and to a lesser extent wild-type signaling through EGFR, enhance the sensitivity to mTOR kinase inhibitors, whereas the presence of PTEN diminishes that requirement. This finding occurs in the absence of evidence that CC214 compounds are more effective at blocking mTORC1/2 signaling in the context of EGFR–PI3K pathway activation. On the contrary, these findings suggest that molecular context exerts significant effects on the dependence of tumor cells on mTOR signaling, such that EGFR and PTEN status could potentially be used to stratify patients for treatment. Notably, these data indicate that PI3K pathway activation may be the point of convergence, suggesting that other PI3K activating lesions in glioblastoma may be critical determinants of response to ATP-competitive mTOR kinase inhibitors.

Furthermore, these results highlight the importance of autophagy as a targeted therapy resistance mechanism in cancer. Our findings are consistent with the work of the Weiss group, showing that PI3K/mTOR kinase inhibition induces autophagy in glioblastoma cells (23). Similarly, our evidences, using genetic and pharmacologic autophagy inhibition, indicate that blocking autophagy could potentially transform mTOR kinase inhibitors into much more successful anticancer agents by converting a cytostatic to a cytotoxic response.

Lastly, the introduction of the DEAL technology to monitor autophagy in single cancer cells, captured from heterogeneous patient-derived tumors, clearly shows that endogenous EGFRvIII is an active promoter of autophagy in mTOR-kinase–inhibited tumors.

Autophagy in cancer has a context-dependent function, representing both, a tumor suppressor role in the early stage of tumor formation, and, conversely, a tumor survival process in response to perturbations, such as chemotherapy treatment (26). As shown by Lock and colleagues, oncogenic Ras-addicted cells have higher level of basal autophagy (27), making the combination of Ras and autophagy inhibitors a potentially efficacious treatment for this cancer phenotype (22). Similarly, PTEN-null glioblastoma cells also exhibit higher basal levels of autophagy and combining PI3K/mTOR kinase inhibitors with chloroquine causes massive tumor cell death in that genetic context. Here, we identify EGFRvIII as a key determinant of mTOR kinase inhibitor sensitivity in glioblastoma, show that CC214-2 can inhibit mTORC1 and mTORC2 signaling in an intracranial tumor model and we show that chloroquine, or genetic autophagy inhibition, dramatically sensitizes glioblastomas to CC214-mediated tumor cell death, providing compelling rationale for combination therapy, coupled to a strategy for stratifying patients most likely to benefit.

Disclosure of Potential Conflicts of Interest

H. Raymon has been employed as a senior director and consultant for Celgene and has ownership interest (including patents). K. Hege is employed as vice president and has ownership interest (including patents). R. Chopra has ownership interest (including patents). T.F. Cloughesy is a consultant and is on the advisory board of Celgene. P. S. Mischel has received commercial research funding and honoraria from

Published OnlineFirst September 12, 2013; DOI: 10.1158/1078-0432.CCR-13-0527

the speakers bureau of Celgene. No potential conflicts of interest were disclosed by the other authors.

Authors' Contributions

Conception and design: B. Gini, D. Guo, G. Villa, S. Xu, W.K. Cavenee, P.S. Mischel

Development of methodology: B. Gini, C. Zanca, D. Guo, G. Villa, S. Zhu, H. Raymon, F.B. Furnari, P.S. Mischel

Acquisition of data (provided animals, acquired and managed patients, provided facilities, etc.): B. Gini, C. Zanca, H. Yang, D. Nathanson, G. Villa, K. Tanaka, I. Babic, D. Akhavan, K. Lin, A. Assuncao, Y. Gu, R. Chopra, T.F. Cloughesy

Analysis and interpretation of data (e.g., statistical analysis, biostatistics, computational analysis): B. Gini, C. Zanca, D. Guo, T. Matsutani, S. Ikegami, G. Villa, D. Shackelford, K. Tanaka, Y. Gu, D.S. Mortensen, H. Raymon, C.D. James, J.R. Heath, K. Hege, T.F. Cloughesy, P.S. Mischel

Writing, review, and/or revision of the manuscript: B. Gini, D. Guo, K. Masui, G. Villa, D. Shackelford, I. Babic, B. Bonetti, D.S. Mortensen, H. Raymon, W.K. Cavenee, F.B. Furnari, C.D. James, G. Kroemer, J.R. Heath, K. Hege, R. Chopra, T.F. Cloughesy, P.S. Mischel

Administrative, technical, or material support (i.e., reporting or organizing data, constructing databases): B. Gini, D. Guo, D. Nathanson, D. Akhavan, A. Assuncao, C.D. James

Study supervision: B. Gini, J.R. Heath, P.S. Mischel

Other (first author contribution): B. Gini

Other (discovery and provision mTOR kinase inhibitors): D.S. Mortensen

Acknowledgments

Flow cytometry was conducted in the UCLA Jonsson Comprehensive Cancer Center (JCCC) and Center for AIDS Research Flow Cytometry Core Facility that is supported by National Institutes of Health awards CA-16042 and AI-28697, and by the JCCC, the UCLA AIDS Institute, and the David Geffen School of Medicine at UCLA; confocal laser scanning microscopy was conducted at the CNSI Advanced Light Microscopy/Spectroscopy Shared Resource Facility at UCLA.

Grant Support

This work is supported by grants from National Institute for Neurological Diseases and Stroke (NS73831), the National Cancer Institute (CA151819), The Ben and Catherine Ivy Foundation, and generous donations from the Ziering Family Foundation in memory of Sigi Ziering. W.K. Cavenee is a Fellow of the National Foundation for Cancer Research.

This work is supported, in part, with funding from NIH-NCRR shared resources grant (CJX1-443835-WS-29646) and NSF Major Research Instrumentation grant (CHE-0722519); NIH (NS072838; to D. Guo); and The European Commission (PIOF-GA-2010-271819; to B. Gini).

The costs of publication of this article were defrayed in part by the payment of page charges. This article must therefore be hereby marked *advertisement* in accordance with 18 U.S.C. Section 1734 solely to indicate this fact.

Received February 27, 2013; revised August 21, 2013; accepted August 22, 2013; published OnlineFirst September 12, 2013.

References

1. Furnari FB, Fenton T, Bachoo RM, Mukasa A, Stommel JM, Stegh A, et al. Malignant astrocytic glioma: genetics, biology, and paths to treatment. Genes Dev 2007;21:2683–710.
2. The Cancer Genome Atlas Network. Comprehensive genomic characterization defines human glioblastoma genes and core pathways. Nature 2008;455:1061–8.
3. Fine B, Hodakoski C, Koujak S, Su T, Saal LH, Maurer M, et al. Activation of the PI3K pathway in cancer through inhibition of PTEN by exchange factor P-REX2a. Science 2009;325:1261–5.
4. Laplante M, Sabatini DM. mTOR signaling in growth control and disease. Cell 2012;149:274–93.
5. Tanaka K, Babic I, Nathanson D, Akhavan D, Guo DL, Gini B, et al. Oncogenic EGFR signaling activates an mTORC2-NF-kappa B pathway that promotes chemotherapy resistance. Cancer Discov 2011;1:524–38.
6. Cloughesy TF, Yoshimoto K, Nghiemphu P, Brown K, Dang J, Zhu S, et al. Antitumor activity of rapamycin in a Phase I trial for patients with recurrent PTEN-deficient glioblastoma. PLoS Med 2008;5:e8.
7. Galanis E, Buckner JC, Maurer MJ, Kreisberg JI, Ballman K, Boni J, et al. Phase II trial of temsirolimus (CCI-779) in recurrent glioblastoma multiforme: a North Central Cancer Treatment Group Study. J Clin Oncol 2005;23:5294–304.
8. Choo AY, Yoon SO, Kim SG, Roux PP, Blenis J. Rapamycin differentially inhibits S6Ks and 4E-BP1 to mediate cell-type-specific repression of mRNA translation. Proc Natl Acad Sci U S A 2008;105:17414–9.
9. Thoreen CC, Chantranupong L, Keys HR, Wang T, Gray NS, Sabatini DM. A unifying model for mTORC1-mediated regulation of mRNA translation. Nature 2012;485:109–13.
10. Mortensen DS, Sapienza J, Lee BG, Perrin-Ninkovic SM, Harris R, Shevlin G, et al. Use of core modification in the discovery of CC214-2, an orally available, selective inhibitor of mTOR kinase. Bioorg Med Chem Lett 2013;23:1588–91.
11. Guo D, Reinitz F, Youssef M, Hong C, Nathanson D, Akhavan D, et al. An LXR agonist promotes glioblastoma cell death through inhibition of an EGFR/AKT/SREBP-1/LDLR-dependent pathway. Cancer Discov 2011;1:442–56.
12. Mortensen DS, Perrin-Ninkovic SM, Harris R, Lee BG, Shevlin G, Hickman M, et al. Discovery and SAR exploration of a novel series of imidazo[4,5-b]pyrazin-2-ones as potent and selective mTOR kinase inhibitors. Bioorg Med Chem Lett 2011;21:6793–9.
13. Shah K, Hingtgen S, Kasmieh R, Figueiredo JL, Garcia-Garcia E, Martinez-Serrano A, et al. Bimodal viral vectors and in vivo imaging reveal the fate of human neural stem cells in experimental glioma model. J Neurosci 2008;28:4406–13.
14. Lee M, Muller F, Aquilanti E, Hu B, DePinho R. Stereotactic orthotopic xenograft injections into the mouse brain. Protocol Exchange 2012 22 Aug.[Epub ahead of print]
15. Mellinghoff IK, Wang MY, Vivanco I, Haas-Kogan DA, Zhu S, Dia EQ, et al. Molecular determinants of the response of glioblastomas to EGFR kinase inhibitors. N Engl J Med 2005;353:2012–24.
16. Gini B, Lovato L, Cianti R, Cecotti L, Marconi S, Anghileri E, et al. Novel autoantigens recognized by CSF IgG from Hashimoto's encephalitis revealed by a proteomic approach. J Neuroimmunol 2008;196:153–8.
17. Bailey RC, Kwong GA, Radu CG, Witte ON, Heath JR. DNA-encoded antibody libraries: a unified platform for multiplexed cell sorting and detection of genes and proteins. J Am Chem Soc 2007;129:1959–67.
18. Thomas HE, Mercer CA, Carnevalli LS, Park J, Andersen JB, Conner EA, et al. mTOR inhibitors synergize on regression, reversal of gene expression, and autophagy in hepatocellular carcinoma. Sci Transl Med 2012;4:139ra84.
19. Kwong GA, Radu CG, Hwang K, Shu CJ, Ma C, Koya RC, et al. Modular nucleic acid assembled p/MHC microarrays for multiplexed sorting of antigen-specific T cells. J Am Chem Soc 2009;131:9695–703.
20. Sarkaria JN, Yang L, Grogan PT, Kitange GJ, Carlson BL, Schroeder MA, et al. Identification of molecular characteristics correlated with glioblastoma sensitivity to EGFR kinase inhibition through use of an intracranial xenograft test panel. Mol Cancer Ther 2007;6:1167–74.
21. Jung CH, Ro SH, Cao J, Otto NM, Kim DH. mTOR regulation of autophagy. FEBS Lett 2010;584:1287–95.
22. Guo JY, Chen HY, Mathew R, Fan J, Strohecker AM, Karsli-Uzunbas G, et al. Activated Ras requires autophagy to maintain oxidative metabolism and tumorigenesis. Genes Dev 2011;25:460–70.
23. Fan QW, Cheng C, Hackett C, Feldman M, Houseman BT, Nicolaides T, et al. Akt and autophagy cooperate to promote survival of drug-resistant glioma. Sci Signal 2010;3:ra81.
24. Yecies JL, Manning BD. Transcriptional control of cellular metabolism by mTOR signaling. Cancer Res 2011;71:2815–20.
25. Thoreen CC, Kang SA, Chang JW, Liu Q, Zhang J, Gao Y, et al. An ATP-competitive mammalian target of rapamycin inhibitor reveals rapamycin-resistant functions of mTORC1. J Biol Chem 2009;284:8023–32.
26. White E. Deconvoluting the context-dependent role for autophagy in cancer. Nat Rev Cancer 2012;12:401–10.
27. Lock R, Roy S, Kenific CM, Su JS, Salas E, Ronen SM, et al. Autophagy facilitates glycolysis during Ras-mediated oncogenic transformation. Mol Biol Cell 2011;22:165–78.